Pentamethylcyclopentadienylrhodaborane Chemistry. Part 3.[1,2] The Reaction of $[\{Rh(\eta^5\text{-}C_5Me_5)Cl_2\}_2]$ with *closo*-$[B_{10}H_{10}]^{2-}$ and *arachno*-$B_{10}H_{12}$-6,9-$(PMe_2Ph)_2$, and the Characterisation of Some Novel Rhodaboranes by *X*-Ray Diffraction * Analysis and Nuclear Magnetic Resonance Spectroscopy

Xavier L. R. Fontaine, Hayat Fowkes, Norman N. Greenwood, John D. Kennedy, and Mark Thornton-Pett
School of Chemistry, University of Leeds, Leeds LS2 9JT

Reaction of the rhodaborane synthon $[\{Rh(\eta^5\text{-}C_5Me_5)Cl_2\}_2]$ with *closo*-$[B_{10}H_{10}]^{2-}$ in dichloromethane solution results in the rapid insertion, in reasonable yield, of a $Rh(\eta^5\text{-}C_5Me_5)$ vertex to give orange, air-stable crystals of $[1\text{-}(\eta^5\text{-}C_5Me_5)\text{-}closo\text{-}1\text{-}RhB_{10}H_{10}]$ (**1**). When methanol is also present the major product (40% yield) is the related orange, air-stable, methoxy derivative $[1\text{-}(\eta^5\text{-}C_5Me_5)\text{-}closo\text{-}1\text{-}RhB_{10}H_9\text{-}2\text{-}(OMe)]$ (**2**). *X*-Ray diffraction analysis of (**2**) established a triclinic unit cell, space group $P\bar{1}$, with a = 1 407.7(2), b = 878.9(1), c = 835.9(2) pm, α = 111.19(1), β = 103.44(1), γ = 92.24(1)°, and Z = 2. Detailed n.m.r. data on (**1**) and (**2**) are also discussed. Reaction of $[\{Rh(\eta^5\text{-}C_5Me_5)Cl_2\}_2]$ with the bis-ligand adduct *arachno*-$B_{10}H_{12}$-6,9-$(PMe_2Ph)_2$ affords yellow, air-stable crystals of the dichloromethane solvate $[7\text{-}(\eta^5\text{-}C_5Me_5)\text{-}nido\text{-}7\text{-}RhB_{10}H_{11}\text{-}8\text{-}Cl\text{-}11\text{-}(PMe_2Ph)]\cdot CH_2Cl_2$ (**3**) [monoclinic, space group $P2_1/n$, with a = 1 520.4(2), b = 1 228.3(3), c = 1 622.3(2) pm, β = 102.24(1)°, and Z = 4]. A notable feature of the structure is the presence of three bridging H atoms in the five-atom RhB_4 open face of the *nido* cluster. Two-dimensional [^{11}B–^{11}B]-COSY, [^{1}H–^{1}H]{^{11}B}-COSY, and ^{1}H-{^{11}B(selective)} n.m.r. experiments revealed further interesting features of this cluster species. Treatment of (**3**) with an excess of the ligand PMe_2Ph in the presence of H_2O or O_2 gave a 63% yield of the novel twelve-vertex *nido*-rhodaoxaborane $[7\text{-}(\eta^5\text{-}C_5Me_5)\text{-}nido\text{-}7,12\text{-}RhOB_{10}H_9\text{-}8\text{-}Cl\text{-}11\text{-}(PMe_2Ph)]$ (**4**). Orange-red, air-stable crystals of (**4**) were monoclinic, space group $P2_1/n$, with a = 867.7(2), b = 1 984.4(4), c = 1 551.8(3) pm, β = 102.08(2)°, and Z = 4. The cluster structure of (**4**) is closely related to that of (**3**) but with the unique oxygen atom replacing two bridging hydrogens in the open face. Detailed n.m.r. data are also presented and discussed.

Part 1 of this series gave an introductory survey of rhodaborane chemistry and reported the reaction of the rhodaborane synthon $[\{Rh(\eta^5\text{-}C_5Me_5)Cl_2\}_2]$ with the nine-vertex substrate *arachno*-$[B_9H_{14}]^-$ to give the straightforward ten-vertex *nido*-6-metalladecaborane $[6\text{-}(\eta^5\text{-}C_5Me_5)\text{-}nido\text{-}6\text{-}RhB_9H_{13}]$ in quantitative yield.[1] Part 2 reported the reaction of this last compound with the tertiary phosphine PMe_2Ph to give a variety of *nido*- and *closo*-rhodaboranes.[2] Here in Part 3 we report chemistry arising from the reactions of $[\{Rh(\eta^5\text{-}C_5Me_5)Cl_2\}_2]$ with the ten-vertex substrates *closo*-$[B_{10}H_{10}]^{2-}$ and *arachno*-$B_{10}H_{12}$-6,9-$(PMe_2Ph)_2$, which lead to some interesting eleven- and twelve-vertex rhodaborane species. Some preliminary aspects of the work have been presented elsewhere.[3,4] Numbering systems for cluster structures encountered in this work are given by (**I**) (ten-vertex *nido* and *arachno*), (**II**) (eleven-vertex *closo* type), (**III**) (eleven-vertex *nido*), and (**IV**) (twelve-vertex *nido* type). Structure (**IV**) is a 'type 7' *nido* twelve-vertex structure as categorised in ref. 5. Note that interconversion among these systems frequently changes the numbering for a particular boron-atom position.

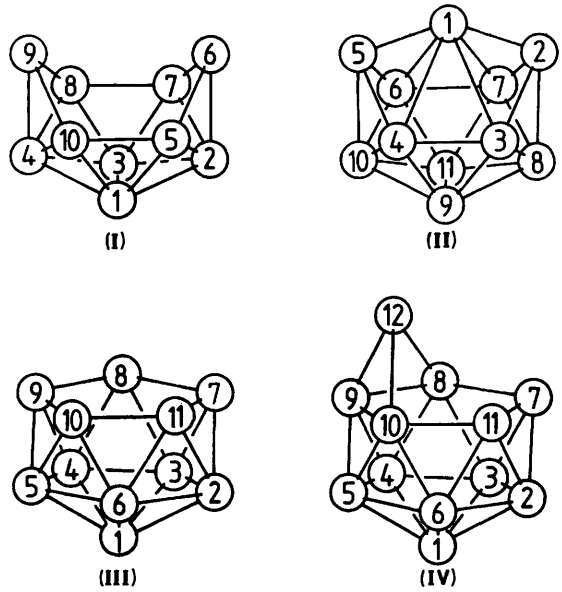

Results and Discussion

Preparation, Structure, and Properties of $[1\text{-}(\eta^5\text{-}C_5Me_5)\text{-}closo\text{-}1\text{-}RhB_{10}H_9X]$ (X = H *or* OMe).—The reaction between $[\{Rh(\eta^5\text{-}C_5Me_5)Cl_2\}_2]$ and *closo*-$[B_{10}H_{10}]^{2-}$ in dichloromethane solution at room temperature gives one principal metallaborane product, an orange crystalline compound (**1**), identified by n.m.r. spectroscopy and by comparison with compound (**2**) (see below) as $[1\text{-}(\eta^5\text{-}C_5Me_5)\text{-}1\text{-}RhB_{10}H_{10}]$ of *closo*-1-metallaundecaborane configuration (**V**). The idealized stoicheiometry is as in equation (1).

* *Supplementary data available:* see Instructions for Authors, *J. Chem. Soc., Dalton Trans.*, 1987, Issue 1, pp. xvii—xx.

$$[\{Rh(\eta^5\text{-}C_5Me_5)Cl_2\}_2] + 2[B_{10}H_{10}]^{2-} \longrightarrow 2[(\eta^5\text{-}C_5Me_5)RhB_{10}H_{10}]\,(\mathbf{1}) + 4Cl^- \quad (1)$$

The measured n.m.r. properties are summarized in Table 1, and the similarity to other[6–10] *closo*-type eleven-vertex 1-metallaundecaboranes of configuration (**V**) readily identifies compound (**1**) as being of the same geometrical and electronic type. The compound was air stable in the solid state, but less robust in solution in the presence of air.

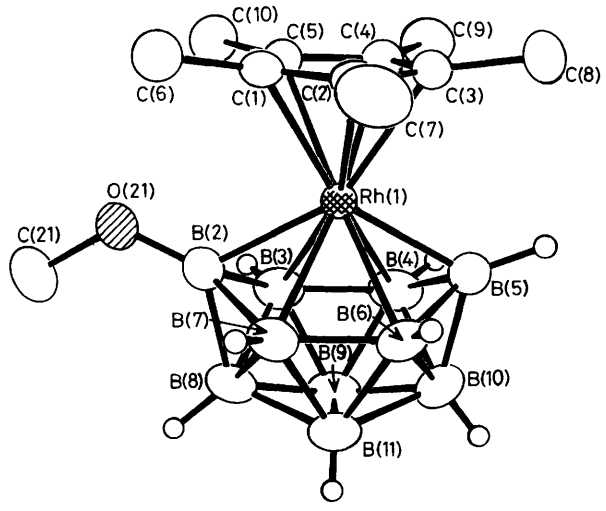

Figure 1. ORTEP drawing of the crystallographically determined molecular structure of [1-(η^5-C_5Me_5)-1-$RhB_{10}H_9$-2-(OMe)] (**2**) with organyl hydrogen atoms omitted for clarity

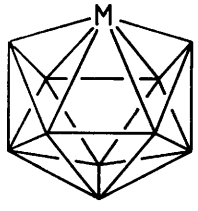

(**V**)

The structural type was confirmed by a single-crystal *X*-ray diffraction analysis of the 2-methoxy substituted analogue [1-(η^5-C_5Me_5)-1-$RhB_{10}H_9$-2-(OMe)] (**2**). This was formed when the above reaction was carried out in methanol rather than dichloromethane [idealized stoicheiometry as in equation (2)]. The orange compound (**2**) is also air stable in the solid state, and appears to be somewhat more stable than compound (**1**) in solution.

$$[\{Rh(\eta^5\text{-}C_5Me_5)Cl_2\}_2] + 2[B_{10}H_{10}]^{2-} + 2\,MeOH \longrightarrow 2[(\eta^5\text{-}C_5Me_5)RhB_{10}H_9(OMe)]\,(\mathbf{2}) + 4Cl^- + 2H_2 \quad (2)$$

The reaction in methanol gave a second yellow compound, at present tentatively identified as the *nido* ten-vertex species [5-(η^5-C_5Me_5)-*nido*-5-RhB_9H_{12}-6-X] (X = Cl or OMe), and we hope to be able to describe this elsewhere along with various other substituted *nido*-5- and *nido*-6-rhoda-, -irida-, -ruthena-, and -osma-decaboranes obtained from a variety of arene–metal–borane anion reaction systems.[9]

The n.m.r. properties of the major product (**2**) showed that it was a 2-substituted derivative of compound (**1**) (Table 1), and this was confirmed by a single-crystal *X*-ray diffraction analysis. A drawing of the molecular structure is in Figure 1, and salient internuclear distances and angles are in Tables 2 and 3 respectively. The $RhB_{10}H_9$ cluster dimensions are very similar to those in the Rh(1)–B(2) hydrogen-bridged eleven-vertex *closo*-type rhodaboranes [1,1-$(PMe_2Ph)_2$-1-$RhB_{10}H_8$-2,5-$(OMe)_2$] and [1,1-$(PMe_2Ph)_2$-1-$RhB_{10}H_8$-2-(OMe)-5-Cl],[6] with the exception that the Rh(1)–B(2) distance, unbridged in compound (**2**), is now some 10 pm shorter than in the previously described[6] Rh(1)–H–B(2) bridged species and is thereby now essentially the same as the Rh(1)–B(5) distance, as expected. The only significant differences are those associated with the methoxy-substituted boron atom B(2) [compared to those of the otherwise equivalent unsubstituted atom B(5)], in that all the interatomic distances to B(2) appear to be some 2—4 pm longer than those to B(5). This could possibly arise from the effect of the electronegativity of the 2-(OMe) group which withdraws electron density from the cluster and thereby reduces the bond orders among the B(2)B(3)B(8)B(7) atoms. It is also of interest that the metal-flanking distances B(3)–B(4) and B(6)–B(7) at *ca.* 170 pm are some 10 pm shorter than the others. The distances from rhodium to B(2) and B(5) are towards the shorter end of

Table 1. Measured n.m.r. properties of [1-(η^5-C_5Me_5)-*closo*-1-$RhB_{10}H_{10}$] (**1**), [1-(η^5-C_5Me_5)-*closo*-1-$RhB_{10}H_9$-2-(OMe)] (**2**) and, for comparison, data[6,8] for [1,1-$(PMe_2Ph)_2$-*closo*-1-$RhB_{10}H_8$-2,5-$(OMe)_2$]

	Compound (**2**) ($CDCl_3$, 297 K)				Compound (**1**) (297 K)				$[(PMe_2Ph)_2Rh\text{-}B_{10}H_8(OMe)_2]$ ($CDCl_3$, 294 K)		
Tentative assignment[a]	δ(11B)/ p.p.m.[b]	Obs. [11B–11B]-COSY45 correlations	δ(1H)/ p.p.m.[c,d]	1J(11B–1H)/ Hz[e]	δ(11B)/ p.p.m.[b] (CD_2Cl_2)	Obs. 11B–11B]-COSY90 correlations (CD_2Cl_2)	δ(1H)/ p.p.m.[c,f] ($CDCl_3$)	1J(11B–1H)/ Hz[e]	δ(11B)/ p.p.m.[b]	δ(1H)/ p.p.m.[c]	Tentative assignment
2	+96.8	(A)w[g] (8)w	+4.62[h]	*i*	+118.8	(3,4,6,7)w (8,10)w	+10.45	175	+90.1	+4.30[h]	2,5
5	+112.1	*j*	+10.10	164							
3,7	+14.3(A)[g]	(2)w (4,6)s (8)s	+2.08	*ca.* 140	+19.9	(2,5)w (8,10)w (9,11)s	+1.66	142	+7.4	+2.41	3,4,6,7
4,6	+9.8	(A)s[g] (10)vw?	+1.39	150							
8	+0.2	(5)w (A)s[g]	+3.49	141	+12.3	(2,5)w (3,4,6,7)w (9,11)s	+4.31	146	+8.5	+3.72	8,10
10	+11.6	(4,6)vw?	+4.08	158							
9,11	+14.3(A)[g]	(2)w (4,6)s (8)s	+2.54	*ca.* 140	+24.4	(3,4,6,7)s (8,10)s	+3.31	145	+3.6	+2.25	9,11

[a] Based on relative intensities, B(2) substituent in compound (**2**), COSY cross-peaks, and parallels in 11B–1H shielding patterns. [b] ±0.5 p.p.m. to low field (high frequency) of $BF_3(OEt_2)$ in $CDCl_3$. [c] Proton resonances related to directly bound boron atom positions by 1H-{11B(selective)} experiments; δ(1H) ± 0.05 p.p.m. to high frequency (low field) of internal $SiMe_4$. [d] δ(1H)(C_5Me_5) at *ca.* +1.65. [e] ±8 Hz; values measured from 11B spectra with line-narrowing to achieve baseline separation of doublet components. [f] δ(1H)(C_5Me_5) at *ca.* +1.73. [g] Note that 11B(9,11) and 11B(3,7) resonances (agglomerate peak 'A') are accidentally coincident. [h] Methoxy resonance. [i] Methoxy substituent position. [j] No cross-peaks observed to this (somewhat broader; $w_{\frac{1}{2}}$ *ca.* 145 Hz) resonance.

Table 2. Interatomic distances (pm) for [1-(η^5-C_5Me_5)-1-$RhB_{10}H_9$-2-(OMe)] (**2**), with estimated standard deviations (e.s.d.s) in parentheses

(*i*) To the rhodium atom			
Rh(1)–B(2)	212.3(5)	Rh(1)–B(5)	210.1(5)
Rh(1)–B(3)	230.2(5)	Rh(1)–B(6)	227.5(5)
Rh(1)–B(4)	229.3(5)	Rh(1)–B(7)	227.9(5)
Rh(1)–C(1)	225.1(4)	Rh(1)–C(4)	223.7(4)
Rh(1)–C(2)	223.6(4)	Rh(1)–C(5)	223.5(4)
Rh(1)–C(3)	226.7(4)		
(*ii*) Boron–boron			
B(2)–B(3)	180.5(6)	B(2)–B(7)	181.2(6)
B(2)–B(8)	173.6(6)	B(5)–B(10)	170.6(6)
B(3)–B(4)	171.7(7)	B(6)–B(7)	171.7(7)
B(3)–B(8)	183.2(6)	B(7)–B(8)	184.7(7)
B(3)–B(9)	176.6(7)	B(7)–B(11)	176.1(6)
B(4)–B(5)	176.5(7)	B(5)–B(6)	177.3(7)
B(4)–B(9)	179.6(6)	B(6)–B(11)	178.7(7)
B(4)–B(10)	184.0(7)	B(6)–B(10)	181.4(7)
B(8)–B(9)	175.4(7)	B(8)–B(11)	177.1(7)
B(9)–B(10)	178.8(7)	B(10)–B(11)	176.4(7)
B(9)–B(11)	176.5(7)		
(*iii*) Boron–hydrogen			
B(3)–H(3)	94(4)	B(7)–H(7)	96(4)
B(4)–H(4)	101(3)	B(6)–H(6)	80(3)
B(8)–H(8)	106(3)	B(10)–H(10)	95(6)
B(9)–H(9)	113(3)	B(11)–H(11)	83(4)
(*iv*) Others			
B(2)–O(21)	133.1(4)	O(21)–C(21)	141.7(4)
C(1)–C(2)	142.2(5)	C(1)–C(6)	150.1(5)
C(2)–C(3)	143.1(4)	C(2)–C(7)	149.8(3)
C(3)–C(4)	141.2(4)	C(3)–C(8)	150.9(5)
C(4)–C(5)	141.8(4)	C(4)–C(9)	150.7(5)
C(5)–C(1)	142.0(4)	C(5)–C(10)	150.7(5)

Table 3. Selected interatomic angles (°) for [1-(η^5-C_5Me_5)-1-$RhB_{10}H_9$-2-(OMe)] (**2**) with e.s.d.s in parentheses

(*i*) About the rhodium atom			
B(2)–Rh(1)–B(3)	47.9(1)	B(2)–Rh(1)–B(7)	48.4(1)
B(2)–Rh(1)–B(4)	89.3(2)	B(2)–Rh(1)–B(6)	90.1(2)
B(2)–Rh(1)–B(5)	122.4(2)		
B(3)–Rh(1)–B(4)	43.9(1)	B(6)–Rh(1)–B(7)	44.3(1)
B(3)–Rh(1)–B(5)	88.3(2)	B(5)–Rh(1)–B(7)	89.0(2)
B(3)–Rh(1)–B(7)	72.8(2)	B(4)–Rh(1)–B(6)	72.7(2)
B(4)–Rh(1)–B(5)	47.1(1)	B(5)–Rh(1)–B(6)	47.6(1)
C(aromatic)–Rh(1)–C(aromatic)	36.5(1)—37.1(1), 61.1(2)—62.1(2)		
(*ii*) Boron–boron–boron			
B(3)–B(2)–B(7)	97.4(3)	B(4)–B(5)–B(6)	99.8(3)
B(2)–B(3)–B(4)	123.8(3)	B(2)–B(7)–B(6)	123.9(3)
B(3)–B(4)–B(5)	123.7(3)	B(5)–B(6)–B(7)	123.4(3)
(*iii*) Others			
B(3)–B(2)–O(21)	130.6(2)	B(7)–B(2)–O(21)	131.6(2)
Rh(1)–B(2)–O(21)	125.0(3)	B(8)–B(2)–O(21)	129.4(3)
B(2)–O(21)–C(21)	122.0(3)		

previously reported ranges,[1-4,6] and the distances to B(3), B(4), B(6), and B(7) at the upper end.

The Rh–η^5-C_5Me_5 geometry is similar to those of the other pentamethylcyclopentadienylrhodaboranes reported in Parts 1[1] and 2[2] and below. The symmetry of the RhB_{10} cluster approximates closely to C_{2v}, and there is no significant tilt between the η^5-C_5Me_5 and B(3)B(4)B(6)B(7) planes (dihedral angle *ca.* 1.0°), in contrast to the cluster asymmetry and 13° tilt observed for the Rh(1)–H–B(2) bridged species reported in ref. 6. As observed for other pentamethylcyclopentadienylrhodaboranes [refs. 1 and 2, and compounds (**3**) and (**4**) below] there is a slight bending of the methyl groups out of the η^5-C_5 plane *away* from the rhodium atom (mean deviation from coplanarity 5.5°). This last behaviour contrasts to that for a variety of metallaboranes and metallacarboranes of first-row transition elements such as iron and cobalt, in which the methyl groups are distorted out of the ring plane *towards* the metal atom.[11]

The idealized C_{2v} closed structure of the metallaborane units of compounds (**1**) and (**2**) [structure (**V**)] introduces interesting questions with respect to the application of the Wade–Williams[12,13] electron-counting and cluster geometry theories, and two views of the electronic structure of this class of compound may be advanced.[14-16] In one of these, it would be held that the Rh(η^5-C_5Me_5) moiety, in the formal oxidation state of rhodium(III), contributes three orbitals and two electrons to the cluster bonding scheme so that the closed structure would have two electrons less than that required for a formal *closo* electron count and would therefore be regarded as 'electron hyperdeficient'. In the second view, it would be held that the Rh(η^5-C_5Me_5) moiety, now in the formal valency state of rhodium(V), contributes four orbitals and four electrons to the cluster bonding scheme, so that the cluster has sufficient electrons for a formal *closo* count but that the metal cluster involvement is thereby exceptional in that it involves four, rather than three, metal valence orbitals in cluster bonding and therefore warrants an '*isocloso*' description.[14-16] In terms of the former interpretation, the 18-electron transition-metal centre would have a six-orbital 'octahedral' type of valence-orbital distribution, with a d^6 core, and in the latter a seven-orbital '3:4 piano-stool' type of valence-orbital distribution with a d^4 core. It may well be that the best simple electronic description involves a resonance hybrid between these two extremes and it will be interesting to see rigorous minimum-presumption molecular-orbital treatments in this area.

Reactions of [{Rh(η^5-C_5Me_5)Cl_2}$_2$] *with arachno*-$B_{10}H_{12}$-6,9-(PMe_2Ph)$_2$: *Characterization of* [7-(η^5-C_5Me_5)-*nido*-7-$RhB_{10}H_{11}$-8-Cl-11-(PMe_2Ph)]·CH_2Cl_2.—A key to answer some of the questions raised in the preceding paragraph would be afforded by an examination of the species [1-(η^5-C_5Me_5)-*closo*-1-$RhB_{10}H_8$-2,5-(PMe_2Ph)$_2$]. This compound would be expected to have a straightforward *closo*-C_{2v} eleven-vertex cluster structure and a *closo* $2n + 2$ electron count, resulting in a metal three-orbital two-electron cluster contribution as in metalladicarbaborane species such as [1,1,1-H(PPh_3)$_2$-1-$IrC_2B_8H_{10}$][17] for which single-crystal *X*-ray diffraction data and assigned ^{11}B n.m.r. spectra have not been reported. To this end we surmised that reaction of [{Rh(η^5-C_5Me_5)Cl_2}$_2$] and the *arachno*-decaborane species $B_{10}H_{12}$-6,9-(PMe_2Ph)$_2$[18] with base might well yield the desired product [equation (3)], although there could also be the possibility of a *closo*-type twelve-vertex cluster formation [equation (4)] related to that recently reported for the synthesis of [(η^5-C_5Me_5)$_2Rh_2SB_9H_8Cl$].[19]

$$[\{Rh(\eta^5\text{-}C_5Me_5)Cl_2\}_2] + 2B_{10}H_{12}(PMe_2Ph)_2 + 4\ \text{base} \xrightarrow{(?)} 2[(\eta^5\text{-}C_5Me_5)RhB_{10}H_8(PMe_2Ph)_2] + 4\ \text{base}\ H^+Cl^- + 2H_2 \quad (3)$$

$$[\{Rh(\eta^5\text{-}C_5Me_5)Cl_2\}_2] + B_{10}H_{12}(PMe_2Ph)_2 \xrightarrow{(?)} [(\eta^5\text{-}C_5Me_5)_2Rh_2B_{10}H_8(PMe_2Ph)_2] + 4HCl \quad (4)$$

In the event, the reaction between [{Rh(η^5-C_5Me_5)Cl_2}$_2$] and $B_{10}H_{12}(PMe_2Ph)_2$ takes the (idealized) stoicheiometry of

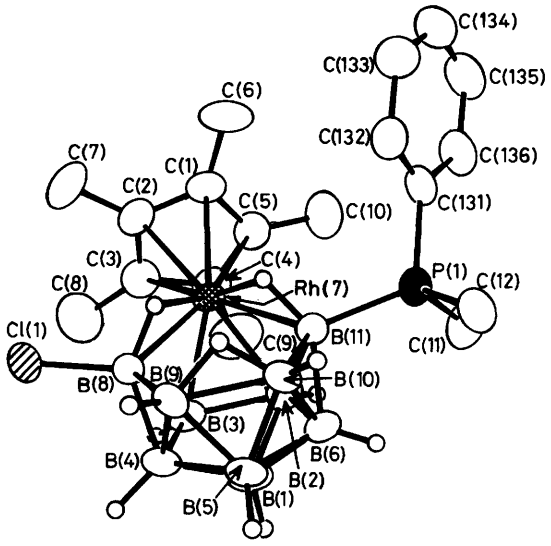

Figure 2. ORTEP drawing of the crystallographically determined molecular structure of $[7\text{-}(\eta^5\text{-}C_5Me_5)\text{-}nido\text{-}7\text{-}RhB_{10}H_{11}\text{-}8\text{-}Cl\text{-}11\text{-}(PMe_2Ph)]\cdot CH_2Cl_2$ (**3**), with organyl hydrogen atoms omitted for clarity [Note that in the preliminary communication of ref. 3 the Figure is wrongly numbered in the B(2)B(3)B(4)B(5)B(6) belt]

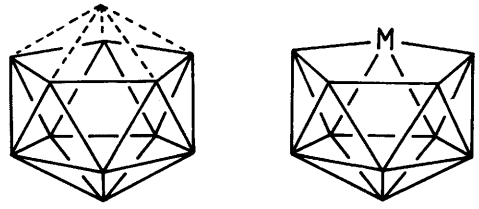

(VI) (VII)

equation (5) to yield the *nido* eleven-vertex species $[(\eta^5\text{-}C_5Me_5)\text{-}RhB_{10}H_{11}Cl(PMe_2Ph)]$ (**3**) as a yellow crystalline compound, air stable in the solid state.

$$[\{Rh(\eta^5\text{-}C_5Me_5)Cl_2\}_2] + 2B_{10}H_{12}(PMe_2Ph)_2 \longrightarrow 2[(\eta^5\text{-}C_5Me_5)RhB_{10}H_{11}Cl(PMe_2Ph)]\ (\mathbf{3}) + 2[PHMe_2Ph]Cl \quad (5)$$

Compound (**3**) was characterized by a single-crystal *X*-ray diffraction analysis of its 1:1 solvate with CH_2Cl_2, all cluster hydrogen atoms being located. A drawing of the molecular structure is in Figure 2, and listings of selected interatomic distances and angles in Tables 4 and 5 respectively.

The basic cluster structure of the compound is seen to be that of a *nido* eleven-vertex monometallaundecaborane formally derived[13] geometrically from the closed triangulated icosahedron by the removal of one vertex [structure (**VI**)]. The metal takes up one of the positions on the open face [structure (**VII**)], with the metal-to-boron distances in the open face being somewhat longer than the other metal-to-boron distances as is generally observed[20] in eleven-vertex *nido*-7-metallaundecaboranes. {It is of interest that the Rh(7)–B(11) distance (*i.e.* to the boron atom bearing the two-electron phosphine ligand) is so long that it is outside previously reported[1–4,6,20,21] ranges, and some 10 pm longer than the Rh(7)–B(8) distance to B(8) which has the one-electron chlorine ligand [*cf.* (**4**) below, Table 7].} The metal atom is somewhat out of the plane defined by the boron atoms in the open face [dihedral angle between the Rh(7)B(8)B(11) and B(8)B(9)B(10)B(11) planes *ca.* 12.6°]. This

Table 4. Selected interatomic distances (pm), with e.s.d.s in parentheses, for $[7\text{-}(\eta^5\text{-}C_5Me_5)\text{-}7\text{-}RhB_{10}H_{11}\text{-}8\text{-}Cl\text{-}11\text{-}(PMe_2Ph)]\cdot CH_2Cl_2$ (**3**)*

(*i*) From the rhodium atom			
Rh(7)–B(2)	225.2(7)	Rh(7)–B(3)	222.1(7)
Rh(7)–B(11)	243.0(7)	Rh(7)–B(8)	231.0(7)
Rh(7)–H(7,11)	182(4)	Rh(7)–H(7,8)	175(4)
Rh(7)–C(1)	224.2(6)	Rh(7)–C(2)	223.2(6)
Rh(7)–C(5)	222.0(6)	Rh(7)–C(3)	221.9(7)
Rh(7)–C(4)	219.1(6)		
(*ii*) Boron–boron			
B(1)–B(2)	178.5(10)	B(1)–B(3)	180.3(9)
B(1)–B(6)	176.3(10)	B(1)–B(4)	173.9(10)
B(1)–B(5)	180.0(10)		
B(2)–B(3)	183.7(10)		
B(2)–B(6)	182.4(9)	B(3)–B(4)	178.9(10)
B(2)–B(11)	182.9(8)	B(3)–B(8)	179.5(9)
B(6)–B(5)	176.8(10)	B(4)–B(5)	180.3(9)
B(6)–B(10)	173.5(9)	B(4)–B(9)	175.3(9)
B(6)–B(11)	175.0(9)	B(4)–B(8)	175.2(9)
B(5)–B(9)	176.0(9)	B(5)–B(10)	177.0(9)
B(10)–B(9)	187.8(9)		
B(10)–B(11)	188.2(8)	B(9)–B(8)	192.3(9)
(*iii*) Boron–hydrogen			
B(1)–H(1)	105(5)		
B(2)–H(2)	111(4)	B(3)–H(3)	118(4)
B(5)–H(5)	111(5)		
B(6)–H(6)	97(6)	B(4)–H(4)	113(5)
B(10)–H(10)	113(4)	B(9)–H(9)	107(4)
B(11)–H(7,11)	121(4)	B(8)–H(7,8)	122(4)
B(10)–H(9,10)	119(4)	B(9)–H(9,10)	126.5(40)
(*iv*) Others			
B(11)–P(1)	194.8(7)	B(8)–Cl(1)	186.2(7)
P(1)–C(11)	177.6(7)	P(1)–C(12)	184.7(7)
P(1)–C(131)	180.4(5)		
C(1)–C(2)	142.7(7)	C(1)–C(6)	150.0(8)
C(2)–C(3)	142.4(8)	C(2)–C(7)	148.9(7)
C(3)–C(4)	143.0(8)	C(3)–C(8)	152.0(9)
C(4)–C(5)	143.7(7)	C(4)–C(9)	148.7(8)
C(5)–C(1)	141.9(7)	C(5)–C(10)	148.4(8)

* Note that the diagram (Figure 1) in the preliminary communication ref. 3 is wrongly numbered.

is as in many other *nido*-7-metallaundecaboranes,[20] but is in contrast to the *nido*-type RhB_{10} subcluster that can be defined in the recently reported macropolyhedral bimetallic 'B-frame' species $[(\eta^5\text{-}C_5Me_5)_2Rh_2B_{17}H_{19}]$[21] in which an agostic Rh–H–B bridge interaction with a second subcluster brings the metal atom somewhat more out of the plane (corresponding dihedral angle *ca.* 21°).[21]

The one-electron chlorine ligand at B(8), together with the two-electron phosphine ligand at B(11) and the three open-face bridging hydrogen atoms, indicate that the rhodium centre can be regarded as being rhodium(III), and as being a straightforward two-electron three-orbital contributor[12] to give the cluster a *nido* $2n + 4$ electron count. In these terms the molecule can be regarded as consisting of a *nido* eleven-vertex 7-metallaundecaborane and a *nido* six-vertex 1-metallahexacarbane cluster conjoined with the metal atom in common. As with a variety of other arene–rhodium[1,2] (and also arene–cobalt)[22–24] boranes, compound (**3**) can also be regarded as having some sandwich character, even though the $\eta^5\text{-}C_5$ and B(2)B(3)B(8)B(11) planes are not quite parallel (dihedral angle 13.0°). Some of this distortion from parallelism is derived from the tilt of the $\eta^5\text{-}C_5Me_5$ grouping away from the B(11)-bound

Table 5. Selected interatomic angles (°) for [7-(η^5-C_5Me_5)-7-$RhB_{10}H_{11}$-8-Cl-11-(PMe_2Ph)]·CH_2Cl_2 (**3**) with e.s.d.s in parentheses *

(*i*) At the metal atom			
B(2)–Rh(7)–B(3)	48.5(2)		
B(2)–Rh(7)–B(8)	82.9(3)	B(3)–Rh(7)–B(11)	82.7(8)
B(2)–Rh(7)–B(11)	45.8(2)	B(3)–Rh(7)–B(8)	46.6(2)
B(11)–Rh(7)–B(8)	87.2(3)		
B(2)–Rh(7)–H(7,8)	100(1)	B(3)–Rh(7)–H(7,11)	102(2)
B(2)–Rh(7)–H(7,11)	74(2)	B(3)–Rh(7)–H(7,8)	77(1)
B(11)–Rh(7)–H(7,8)	81(1)	B(8)–Rh(7)–H(7,11)	85(1)
B(11)–Rh(7)–H(7,11)	29(1)	B(8)–Rh(7)–H(7,8)	31(1)
H(7,8)–Rh(7)–H(7,11)	66(2)		
C(aromatic)–Rh(7)–C(aromatic)	37.1(2)—38.0(2), 62.0(3)–63.5(3)		
(*ii*) Rhodium–boron–boron			
Rh(7)–B(2)–B(1)	118.1(4)	Rh(7)–B(3)–B(1)	118.8(4)
Rh(7)–B(2)–B(3)	64.9(3)	Rh(7)–B(3)–B(2)	66.6(3)
Rh(7)–B(2)–B(6)	120.0(4)	Rh(7)–B(3)–B(4)	118.8(4)
Rh(7)–B(8)–B(3)	64.1(3)	Rh(7)–B(11)–B(2)	62.0(3)
Rh(7)–B(8)–B(4)	116.1(4)	Rh(7)–B(11)–B(6)	114.6(4)
Rh(7)–B(8)–B(9)	113.8(4)	Rh(7)–B(11)–B(10)	114.0(4)
(*iii*) Boron–boron–boron			
B(3)–B(2)–B(11)	114.1(4)	B(2)–B(3)–B(8)	112.4(4)
B(3)–B(8)–B(9)	104.7(4)	B(2)–B(11)–B(10)	105.6(4)
B(8)–B(9)–B(10)	113.0(4)	B(11)–B(10)–B(9)	109.9(4)
Other B–B–B(acute)	57.2(4)—66.5(4),	B–B–B(obtuse)	104.9(4)—115.9(5)
(*iv*) Others			
Rh(7)–B(8)–Cl(1)	119.3(3)	Rh(7)–B(11)–P(1)	128.9(3)
B(9)–B(8)–Cl(1)	121.3(4)	B(10)–B(11)–P(1)	113.7(4)
Rh(7)–H(7,8)–B(8)	101(2)	Rh(7)–H(7,11)–B(11)	105(3)
B(9)–H(9,10)–B(10)	100(3)		

* Horizontal rows comprise angles that would be equal if the molecule conformed to mirror-plane symmetry [through Rh(7)C(5)C(8)H(9,10)-B(1)B(5)] to which it approximates.

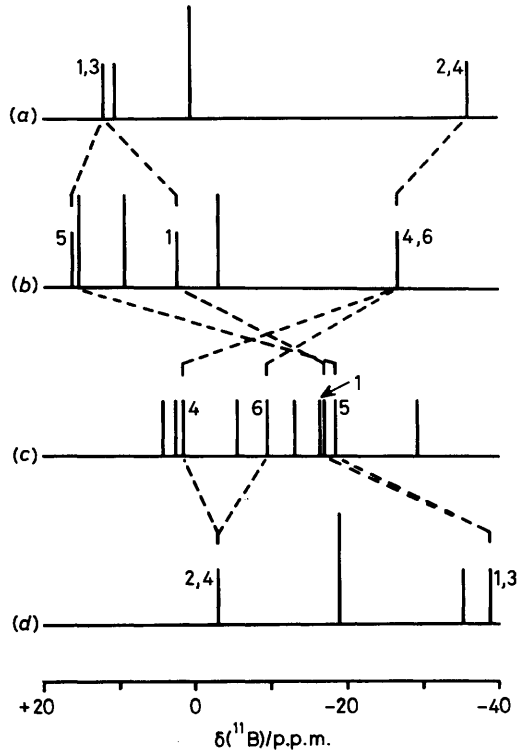

Figure 3. Stick-diagram of the ^{11}B n.m.r. chemical shifts for (*a*) *nido*-$B_{10}H_{14}$, (*b*) [7,7-(PMe_2Ph)$_2$-*nido*-7-$PtB_{10}H_{12}$], (*c*) [7-(η^5-C_5Me_5)-*nido*-7-$RhB_{10}H_{11}$-8-Cl-11-(PMe_2Ph)] (**3**), and (*d*) *arachno*-$B_{10}H_{12}$-6,9-(PMe_2Ph)$_2$. Note that there is a difference in numbering for particular atom positions between the ten-vertex clusters [structure (**I**)] and the eleven-vertex metallaboranes [structure (**III**)]. There is an inversion of the shielding pattern between the *nido* and *arachno* ten-vertex binary borane species, and it can be seen that the ten-boron units of the two metallaboranes can be regarded as being successive intermediates along this progression

phosphine ligand, the distortion presumably being sterically induced to at least some extent. There is also some bending of the arene-bound methyl groups away from the metal atom (mean deviation from planarity 5.33°), as also observed from compound (**2**) above (mean deviation 5.50°), compound (**4**) below (mean deviation 4.83°), and the other previously reported[1,2,21] pentamethylcyclopentadienylrhodaboranes (deviations 2.56—4.80°). As mentioned previously,[2] this contrasts to the behaviour for related metallaboranes and metallacarboranes of first-row transition elements such as cobalt and iron, in which the methyl groups are distorted out of the η^5-C_5 ring plane *towards* the metal atom.[11]

Of particular interest in compound (**3**), however, is the presence and location of the three bridging hydrogen atoms on the open face. Although many *nido*-7-metallaundecaboranes have been reported, with some twenty different types of metal atoms,[20] all these have only two bridging hydrogen atoms that take the (static) H(8,9) and H(10,11) positions on the cluster [structure (**VIII**)]. Apart from some very recently identified ruthenium, molybdenum, and tungsten derivatives,[25,26] the only possible exception to this generalization is a neutral nickelaborane species identified as [7-(η^5-C_5H_5)-*nido*-7-$NiB_{10}H_{13}$],[27] but the similarity of the n.m.r. properties of this entity to those of doubly-bridged species including its own doubly-bridged anionic congener [7-(η^5-C_5H_5)-*nido*-7-$NiB_{10}H_{12}$]$^-$ suggests that it may not in fact take the same triply bridged configuration (**IX**) as the *nido*-7-rhodaundecaborane (**3**) which has a markedly different ^{11}B n.m.r. shielding pattern (see Table 6 and Figure 3).

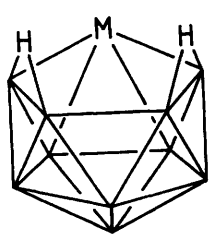

(**VIII**)

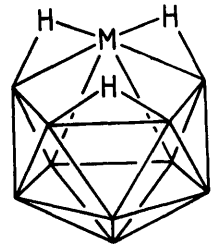

(**IX**)

In compound (**3**) these three bridging hydrogen atoms are fluxional, with rapid mutual exchange occurring at ambient temperature in solution, variable-temperature ^1H-{^{11}B} n.m.r. spectroscopy (footnote *o* in Table 6) giving an activation energy $\Delta G^{\ddagger}$ of *ca.* 31 kJ mol^{-1} for this process at 169 K. This fluxionality together with the crystallographically established bridging-hydrogen atom configuration (**IX**) has implications for the interpretation of the structure of the well known isoelectronic and isolobal *nido*-undecaborane anion [$B_{11}H_{14}$]$^-$ as described elsewhere.[3]

As mentioned in the last paragraph, the more detailed cluster n.m.r. shielding behaviour (Table 6), for which we were able to make reasonably certain assignments of the ^{11}B and ^1H resonances using two-dimensional [^{11}B–^{11}B]-COSY[28–30] and [^1H–^1H]{^{11}B}-COSY,[31] allied with ^1H-{^{11}B(selective)},[32,33] n.m.r. spectroscopy, showed a completely different pattern to

Table 6. Measured n.m.r. properties of [7-(η^5-C_5Me_5)-*nido*-7-$RhB_{10}H_{11}$-8-Cl-11-(PMe_2Ph)] (**3**) in CD_2Cl_2 soluton at 294 K

Tentative assignment[a]	$\delta(^{11}B)$/p.p.m.[b]	Obs. [^{11}B–^{11}B]-COSY45 correlations[c]	$\delta(^1H)$/p.p.m.[d]	Obs. [^1H–^1H] correlations[e]	$^1J(^{11}B$–$^1H)$/Hz[f]
1	−17.0(A)[g]	(2)s (3)s (4)s (5)s (6)s	+1.50	(B)w (2)w (3)w (4)s	(137)
2	+2.5	(A)s (6)w (11)s	+2.16	(1)w	128
3	+4.1[h]	(A)s (2)w? (8)s	+2.22	(1)w (4)s	139
4	+1.6	(A)s (5)s (8)s (9)vw	+2.82	(B)s (3)s	140
5	−18.5	(A)s (4)s (6)s (9)vw	+1.94(B)[i]	(1)w (4)s	143
6	−9.6	(A)s (2)w (5)s (11)s	+1.98[j](B)[i]	(1)w	136
7	Rh		1.60[k]		
8	−5.6	(2)s (4)s (9)vw?	*l*		
9	−13.4	(4)vw (5)vw (8)vw?	+1.92(B)[i]	(4)s	126
10	−16.9(A)[g]	(5)s (6)s (11)w	+1.97(B)[i]		(137)
11	−29.2[m]	(A)w (2)s (6)s	*n*		
7,8					
7,11			−7.29[o,p]	(B)w	
9,10			−6.47[o,q]		

[a] Based on [^{11}B–^{11}B]- and [^1H–^1H]-COSY correlations, ^1H-{^{11}B(selective)} experiments, and B(8) and B(11) substituent positions. [b] ±0.5 p.p.m. to low field (high frequency) of $BF_3(OEt_2)$ in $CDCl_3$. [c] Measured under conditions of ^1H (broad-band) decoupling. [d] Proton resonances related to directly bound boron atom positions by ^1H-{^{11}B(selective)} experiments; $\delta(^1H)$ ±0.05 p.p.m. to high frequency (low field) of internal $SiMe_4$. [e] Measured under conditions of ^{11}B(broad-band) decoupling. [f] ±8 Hz; values measured from ^{11}B spectra with line-narrowing to achieve baseline separation of doublet components; values in parentheses not measureable accurately because of overlapping resonances (see footnote *g*). [g] Note that $^{11}B(1)$ and $^{11}B(10)$ resonances (agglomerate peak 'A') are not resolved in the [^{11}B–^{11}B]-COSY spectrum. [h] This value was erroneously transcribed as +14.2 in the preliminary communication of ref. 3. [i] Note that $^1H(5)$, $^1H(6)$, $^1H(9)$, and $^1H(10)$ resonances (agglomerate peak 'B') are not resolved in the [^1H–^1H]-COSY spectrum. [j] Doublet, *ca.* 17 Hz ascribed to $^1J(^{103}Rh$–$^1H)$. [k] C_5Me_5 resonance position (at 253 K). [l] Cl-substituted site. [m] Doublet, *ca.* 125 Hz, ascribed to $^1J(^{31}P$–$^{11}B)$. [n] PMe_2Ph-substituted site; P-methyl resonances at $\delta(^1H)$ +1.77 [$^2J(^{31}P$–C–$^1H)$ 11.8 Hz] and +1.71 [$^2J(^{31}P$–C–H) 11.9 Hz] p.p.m. (at 253 K); $\delta(^{31}P)$ −2.4 p.p.m. (broad quartet) to high frequency (low field) of 85% H_3PO_4. [o] Measured at 161 K; coalescence of $\delta(^1H)$ −7.29 and −6.47 p.p.m. resonances occurs at 169 K at 9.4 T (400 MHz), giving $\Delta G^{\ddagger}_{169}$ *ca.* 31 kJ mol^{-1}; at 294 K, $\delta(^1H)$ is at −6.70 p.p.m. (3 H). [p] Intensity 2 H; separate ^1H resonances not distinguished at 161 K, presumably due to exchange. [q] Intensity 1 H.

that for a doubly-bridged species. These differences are exemplified in Figure 3, which includes data for *nido*-$B_{10}H_{14}$,[34] *arachno*-$B_{10}H_{12}$-6,9-($PMe_2Ph)_2$,[18] and the doubly bridged *nido*-7-metallaundecaborane [7,7-($PMe_2Ph)_2$-7-$PtB_{10}H_{12}$][32] for comparison. These species are included to emphasize the essential inversion of the ^{11}B nuclear shielding pattern that occurs when compound (**3**) is compared with the *doubly* bridged *nido*-7-metallaundecaboranes [due allowance being made for the deshielding effect of the electronegative chlorine substituent on B(8) in compound (**3**)]. This inversion is characteristic of a *nido* ⟶ *arachno* ten-vertex transition,[34–36] and the positions of the two metallaboranes on this progression suggest that the bonding character of the ten-boron residue has progressed much more from *nido* towards *arachno* in compound (**3**) than it has in doubly-bridged species such as the platinaborane in which the incipient ten-boron *arachno* character is much more localized in the metal-to-boron interface. We have contemporaneously observed a similar crossover effect in the comparison of a series of doubly and triply hydrogen-bridged *nido*-7-molybda- and tungsta-undecaboranes.[26] Structures (**X**)—(**XIII**) illustrate the relationship between (*a*) these postulated valence-bond contributions to the electronic structures of the two metallaborane types (**XI**) and (**XII**) and (*b*) the *nido* and *arachno* electronic structures of the binary borane ten-boron cluster species $B_{10}H_{14}$ and $[B_{10}H_{14}]^{2-}$ [structures (**X**) and (**XIII**) respectively]. As with the metal-to-borane bonding in compounds (**1**) and (**2**) mentioned above, it will be useful to have rigorous minimum-presumption molecular-orbital treatments of these binding modes.

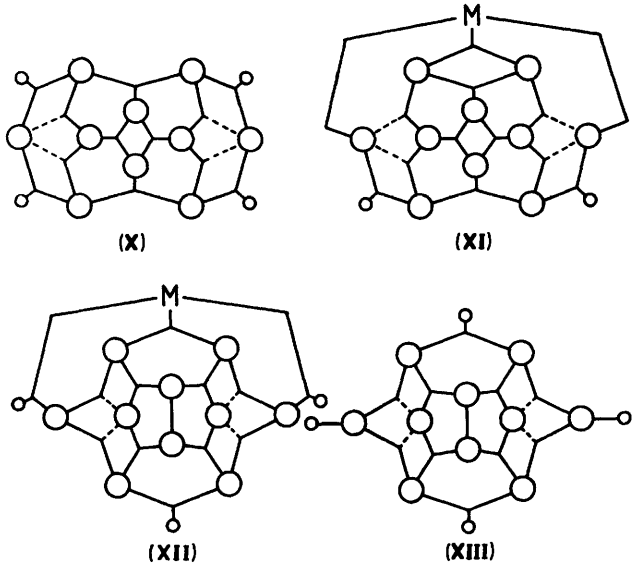

(**X**) (**XI**) (**XII**) (**XIII**)

Preparation and Characterization of the Novel Twelve-vertex nido-*Rhodaoxaborane* [(η^5-C_5Me_5)$RhOB_{10}H_9Cl(PMe_2Ph)$]. —A further approach to the key bis-substituted *closo* species [(η^5-C_5Me_5)$RhB_{10}H_8(PMe_2Ph)_2$] is, in principle, afforded by treatment of compound (**3**) with an excess of PMe_2Ph. The reasoning was that this might induce HCl elimination followed by dihydrogen loss and cluster closure [equation (6)]; this would have some parallels to the reported PMe_2Ph-induced closure of the *nido* ten-vertex rhodaborane [6-(η^5-C_5Me_5)-*nido*-6-RhB_9H_{13}] to give the ten-vertex bis(phosphine) *closo* species [2-(η^5-C_5Me_5)-2-RhB_9H_7-3,10-($PMe_2Ph)_2$] [equation (7)].[2]

$$[(\eta^5\text{-}C_5Me_5)RhB_{10}H_{11}Cl(PMe_2Ph)]\ (\mathbf{3}) + 2PMe_2Ph \xrightarrow{(?)} [(\eta^5\text{-}C_5Me_5)RhB_{10}H_8(PMe_2Ph)_2] + [PHMe_2Ph]Cl + H_2 \quad (6)$$

$$[(\eta^5\text{-}C_5Me_5)RhB_9H_{13}] + 2PMe_2Ph \longrightarrow [(\eta^5\text{-}C_5Me_5)RhB_9H_7(PMe_2Ph)_2] + 3H_2 \quad (7)$$

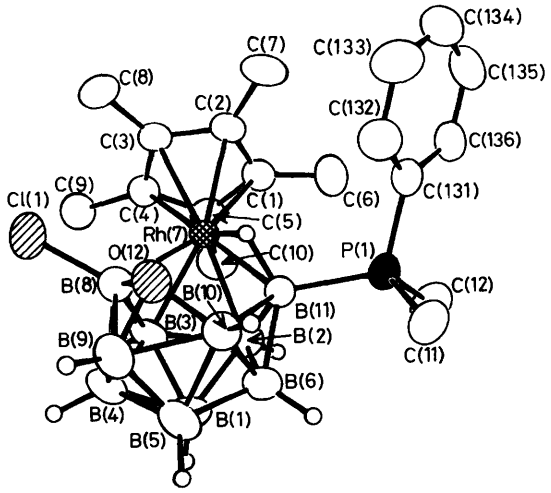

Figure 4. ORTEP drawning of the crystallographically determined molecular structure of [7-(η^5-C_5Me_5)-*nido*-7,12-$RhOB_{10}H_9$-8-Cl-11-(PMe_2Ph)] (**4**), with organyl hydrogen atoms omitted for clarity

Table 7. Interatomic distances (pm) for [7-(η^5-C_5Me_5)-7,12-$RhOB_{10}H_9$-8-Cl-11-(PMe_2Ph)] (**4**) with e.s.d.s in parentheses

(*i*) From the rhodium atom			
Rh(7)–B(2)	218.9(6)	Rh(7)–B(3)	218.8(6)
Rh(7)–B(11)	220.9(6)	Rh(7)–B(8)	232.7(6)
Rh(7)–H(7,11)	177.6(20)		
Rh(7)–C(1)	220.0(5)	Rh(7)–C(2)	222.7(5)
Rh(7)–C(5)	218.6(5)	Rh(7)–C(3)	225.2(5)
Rh(7)–C(4)	221.0(5)		
(*ii*) Boron–boron			
B(1)–B(2)	181.3(9)	B(1)–B(3)	177.4(8)
B(1)–B(6)	178.8(8)	B(1)–B(4)	174.4(9)
B(1)–B(5)	174.7(9)		
B(2)–B(3)	182.1(8)		
B(2)–B(6)	179.7(8)	B(3)–B(4)	179.4(8)
B(2)–B(11)	177.0(8)	B(3)–B(8)	179.5(8)
B(6)–B(5)	177.4(8)	B(4)–B(5)	175.4(9)
B(6)–B(10)	178.9(8)	B(4)–B(9)	174.6(9)
B(6)–B(11)	172.2(7)	B(4)–B(8)	188.9(8)
B(5)–B(9)	171.8(9)	B(5)–B(10)	186.1(8)
B(10)–B(9)	191.7(8)		
B(10)–B(11)	201.2(9)	B(9)–B(8)	199.9(8)
(*iii*) Boron–hydrogen			
B(1)–H(1)	109.7(14)		
B(2)–H(2)	109.2(19)	B(3)–H(3)	121.4(17)
B(5)–H(5)	113.7(21)		
B(6)–H(6)	111.2(19)	B(4)–H(4)	112.5(22)
B(10)–H(10)	110.6(18)	B(9)–H(9)	120.7(22)
B(11)–H(7,11)	124.5(15)		
(*iv*) Others			
B(11)–P(1)	194.7(6)	B(8)–Cl(1)	182.3(6)
B(8)–O(12)	152.1(7)	B(10)–O(12)	153.5(7)
B(9)–O(12)	147.5(7)		
P(1)–C(11)	181.3(6)	P(1)–C(12)	179.3(6)
P(1)–C(131)	179.6(4)		
C(1)–C(2)	141.6(6)	C(1)–C(6)	150.9(7)
C(2)–C(3)	143.5(6)	C(2)–C(7)	149.9(6)
C(3)–C(4)	142.1(6)	C(3)–C(8)	150.9(7)
C(4)–C(5)	143.4(6)	C(4)–C(9)	150.7(7)
C(5)–C(1)	143.3(6)	C(5)–C(10)	149.9(6)

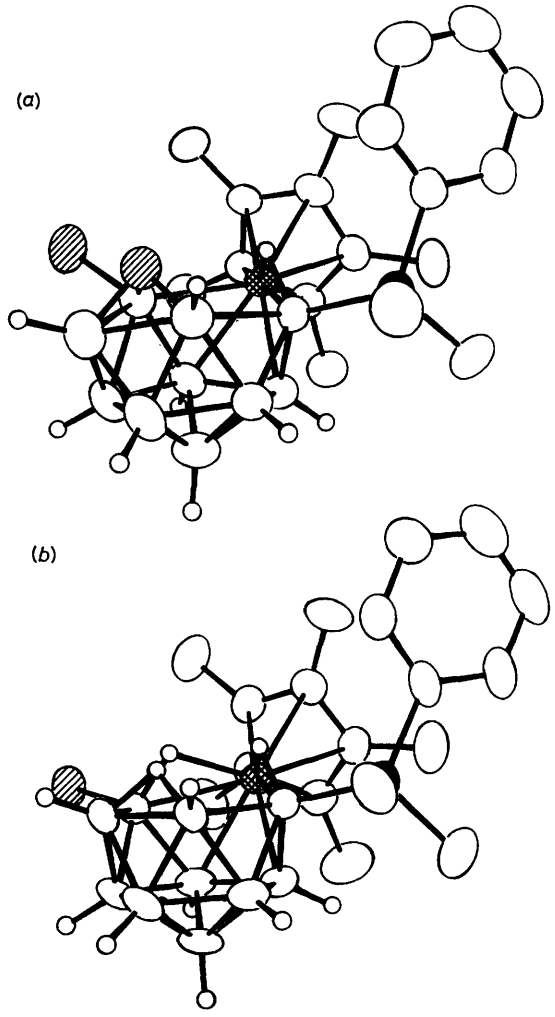

Figure 5. ORTEP drawings of the molecular structures of (*a*) [(η^5-C_5Me_5)$RhOB_{10}H_9Cl$(PMe_2Ph)] (**4**) and (*b*) [(η^5-C_5Me_5)$RhB_{10}H_{11}$-Cl(PMe_2Ph)] (**3**) in orientations selected to show the extreme similarity of the structural configurations

However, compound (**3**) with excess PMe_2Ph in dichloromethane solution gave instead a new, orange-red, air-stable metallaborane species (**4**) which was identified by single-crystal *X*-ray diffraction analysis and n.m.r. spectroscopy as a novel rhodaoxaborane of formulation [(η^5-C_5Me_5)$RhOB_{10}H_9Cl$-(PMe_2Ph)].[4] Although preliminary experiments have indicated that (**4**) probably arises from trace quantities of moisture in the system [idealized equation (8)], we have not yet disproved the possibility that elemental dioxygen may be involved [*e.g.* equation (9)] and also the role of PMe_2Ph, which appears to accelerate the formation of compound (**4**) somewhat, is not yet clear. We are at present attempting to define these conditions more precisely, and hope to report on this and related implications in the future. Meanwhile, because of the unusual nature of the species, we currently present details of its structure and n.m.r. characteristics.

$$[(\eta^5\text{-}C_5Me_5)RhB_{10}H_{11}Cl(PMe_2Ph)]\ (\mathbf{3}) + H_2O \longrightarrow [(\eta^5\text{-}C_5Me_5)RhOB_{10}H_9Cl(PMe_2Ph)]\ (\mathbf{4}) + 2H_2 \quad (8)$$

$$[(\eta^5\text{-}C_5Me_5)RhB_{10}H_{11}Cl(PMe_2Ph)]\ (\mathbf{3}) + O_2 \xrightarrow{(?)} [(\eta^5\text{-}C_5Me_5)RhOB_{10}H_9Cl(PMe_2Ph)]\ (\mathbf{4}) + H_2O \quad (9)$$

Table 8. Selected interatomic angles (°) for [7-(η^5-C_5Me_5)-7,12-$RhOB_{10}H_9$-8-Cl-11-(PMe_2Ph)] (**4**) with e.s.d.s in parentheses

(*i*) At the metal atom			
B(2)–Rh(7)–B(3)	49.2(2)		
B(2)–Rh(7)–B(8)	81.9(3)	B(3)–Rh(7)–B(11)	82.6(2)
B(2)–Rh(7)–B(11)	47.5(2)	B(3)–Rh(7)–B(8)	46.7(2)
B(2)–Rh(7)–H(7,11)	80.6(5)	B(3)–Rh(7)–H(7,11)	101.3(7)
B(8)–Rh(7)–H(7,11)	75.4(8)	B(11)–Rh(7)–H(7,11)	34.3(4)
C(aromatic)–Rh(7)–C(aromatic)	37.1(1)—38.1(1), 62.3(2)—63.0(2)		
(*ii*) Rhodium–boron–boron			
Rh(7)–B(2)–B(1)	119.1(4)	Rh(7)–B(3)–B(1)	121.1(4)
Rh(7)–B(2)–B(3)	65.4(3)	Rh(7)–B(3)–B(2)	65.5(3)
Rh(7)–B(2)–B(6)	114.9(3)	Rh(7)–B(3)–B(4)	129.3(4)
Rh(7)–B(8)–B(3)	62.5(3)	Rh(7)–B(11)–B(2)	65.7(3)
Rh(7)–B(8)–B(4)	117.0(3)	Rh(7)–B(11)–B(6)	117.3(3)
Rh(7)–B(8)–B(9)	134.5(2)	Rh(7)–B(11)–B(10)	108.8(3)
(*iii*) Boron–boron–boron			
B(3)–B(2)–B(11)	107.8(4)	B(2)–B(3)–B(8)	110.0(4)
B(3)–B(8)–B(9)	105.7(4)	B(2)–B(11)–B(10)	103.7(4)
B(8)–B(9)–B(10)	83.1(4)	B(11)–B(10)–B(9)	126.5(4)
(*iv*) Others			
B(8)–O(12)–B(10)	116.5(4)		
B(8)–O(12)–B(9)	83.7(4)	B(9)–O(1)–B(10)	79.1(4)
Rh(7)–B(8)–Cl(1)	115.2(3)	Rh(7)–B(11)–P(1)	128.5(3)
B(9)–B(8)–Cl(1)	107.2(3)	B(10)–B(11)–P(1)	115.2(3)
Rh(7)–B(8)–O(12)	101.3(3)		
O(12)–B(8)–Cl(1)	109.2(4)		
Rh(7)–H(7,11)–B(11)	92.3(9)		

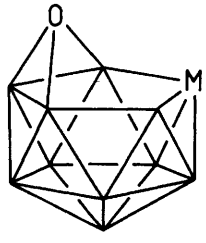

(XIV)

A drawing of the crystallographically determined molecular structure of compound (**4**) is in Figure 4, and selected interatomic distances and angles are in Tables 7 and 8 respectively. It is immediately evident that the gross molecular configuration of compound (**4**) is remarkably similar to that of its precursor (**3**) (Figure 5 affords a comparison). However, although both crystallize monoclinically [space group $P2_1/n$ and $Z = 4$] they are not isomorphous. Compound (**3**), crystallising as a CH_2Cl_2 solvate, has $a = 1\,520.4(2)$, $b = 1\,228.3(3)$, $c = 1\,622.3(2)$ pm, and $\beta = 102.24(1)°$, and the non-solvated rhodaoxaborane (**4**) has $a = 867.7(2)$, $b = 1\,984.4(4)$, $c = 1\,551.8(3)$ pm, and $\beta = 102.08(2)°$. The principal difference in molecular structure is that (**4**) has no bridging hydrogen atoms at the Rh(7)–B(8) and B(9)–B(10) positions, but has instead an oxygen atom bound contiguously to B(8), B(9), and B(10), the resulting $RhOB_{10}$ cluster atoms thereby constituting an open twelve-vertex *nido*-type configuration [(**IV**) and (**XIV**)] ('type 7' *nido* twelve-vertex according to Grimes' presentation [5]). That the atom at position 12 is indeed oxygen rather than another first-row element is reasonably inferred from (*a*) the short interatomic distances to the adjacent boron atoms B(8), B(9), and B(10), (*b*) unacceptably low thermal parameters (< 20 pm^2 compared to *ca.* 50 pm^2 for the other boron cage atoms) when the atom was refined as carbon or boron, and (*c*) the absence, in Fourier difference syntheses, of any additional electron density about atom 12 that would have corresponded to hydrogen atoms expected if the atom were boron or carbon (all other hydrogen atoms being readily located in the structural analysis). This conclusion tends to be confirmed by (*d*) the ^{11}B and ^1H n.m.r. spectra of the compound (Table 9 below), which show that only ten boron atoms were present, together with eight *exo*-terminal BH protons and one bridging Rh–H–B proton.

There is little gross perturbation of the cluster geometry of (**3**) upon the incorporation of the oxygen atom to give (**4**). There is a slight dip in the Rh(7)B(8)B(9)B(10)B(11) open face to accommodate it [Rh(7)B(8)B(10)B(11)/B(8)B(9)B(10) dihedral angle 13.8° in (**4**) compared to 6.8° in (**3**)] but there are only minor changes in interatomic distances to the oxygen-bound B(8), B(9), and B(10) atoms. Thus the distance Rh(7)–B(8), although now *without* the Rh–H–B bridge, is essentially the same as the equivalent (bridged) distance in compound (**3**), and the oxygen-faced distances B(8)–B(9) and B(9)–B(10) are also very similar in both compounds. There does however appear to be a *ca.* 10 pm lengthening of the B(5)–B(10) and B(4)–B(8) distances to the outer two boron atoms involved in binding the oxygen atom to the cluster. Interestingly, the principal geometric and electronic change seems to be at the P-substituted B(11) atom distal to the oxygen vertex. Although the distance B(11)–P(1) (which also happens to be at the extreme higher end of reported ranges [20] for pendant phosphine ligands on metallaborane clusters) is essentially identical to the equivalent distance in compound (**3**), the distance Rh(7)–B(11), which is still associated with a Rh–H–B bridge, is some 20 pm *shorter* than in compound (**3**), whereas B(10)–B(11) to the adjacent open-face boron atom is some 10 pm *longer*. That this may be associated with fundamental electronic changes is suggested not only by the dramatic 50 p.p.m. change in $\delta(^{11}B)$ for this phosphine-bound B(11) atom between compounds (**3**) and (**4**) [a move from the extreme high-field to the extreme low-field end of the spectrum (Tables 6 and 9)], but also by the $\delta(^{11}B)$ changes of up to *ca.* 25 p.p.m. for the other boron nuclei in the cluster, resulting in a chemical shift pattern that now bears no readily discernible relationship to those of the ten-boron units of which the n.m.r. shielding patterns are illustrated in Figure 3 above.

The incidence of a cluster-bound oxygen atom in compound (**4**) is unique in that it is the first polyhedral boron-containing compound reported that has a contiguous oxygen bound solely to boron atoms in the cluster. The sole other example of a contiguous polyhedral oxaborane species, the ten-vertex *nido* compound [2-(η^5-C_5Me_5)-*nido*-2,6-$FeOB_8H_{10}$],[10] has the oxygen atom bound to the cluster metal atom as well as to boron although in both species the oxygen cluster-connectivity is three. It may also be noted that compound (**4**) is the first open-faced twelve-vertex metallaborane cluster reported that does not contain carbon atoms in the cluster; moreover the reaction which results in its formation is also extremely unusual by virtue of the facile uptake of oxygen by the cluster.*

The cluster n.m.r. parameters (chemical shifts and coupling constants) measured for compound (**4**) are given in Table 9. As with the non-oxygenated precursor (**3**), reasonable assignments were made using multidimensional [28–31] and multiple-resonance spectroscopy.[32,33] An interesting feature in addition to the dramatic $^{11}B(11)$ shielding change already mentioned is

* Other related examples are beginning to emerge from rhodaborane systems: *e.g.* the formation of [9,9′-μ-O-{5-(η^5-C_5Me_5)-*nido*-5-RhB_9H_{12}}$_2$], X. L. R. Fontaine, H. Fowkes, N. N. Greenwood, J. D. Kennedy, P. MacKinnon, and M. Thornton-Pett, unpublished work, 1984—1986.

Table 9. Measured n.m.r. properties of [7-(η^5-C_5Me_5)-*nido*-7,12-$RhOB_{10}H_9$-8-Cl-11-(PMe_2Ph)] (**4**) in CD_2Cl_2 solution at 294 K

Tentative assignment[a]	$\delta(^{11}B)$/p.p.m.[b]	Obs. [^{11}B–^{11}B]-COSY90 correlations[c] ($CDCl_3$, 328 K)	$\delta(^1H)$/p.p.m.[d]	Obs. [^1H–^1H] correlations[e]	$^1J(^{11}B$–$^1H)$/Hz[f]
1	+5.9(A)[g]	(4)w (5)w (6)w (9)s	+3.06	(2)s (3)w? (4)s (5)s (6)vw	(110)
2	−4.4	(3)vw (11)s	+1.34	(1)s (3)s (6)s	(120)
3	+10.7	(A)s (2)vw	+2.96	(1)w? (2)s (4)s (9)vw?	(140)
4	−6.7	(A)w	+2.69	(1)s (3)s (5)s (9)s	140
5	−1.3	(A)w	+3.40	(1)s (4)s (6)s (9)w? (11)s	139
6	−3.8	(A)w (11)s	+2.23[h]	(1)vw (5)s	(100)
7	Rh		+1.62[i]		
8	+5.5(A)[g]	(4)w (5)w (6)w (9)s	*j*		
9	+12.1		+3.28	(3) vw? (4)s (5)w?	(180)
10	−12.9		+1.94	(5)s	153
11	+21.1[k]	(2)s (6)s	*l*		87[m]
7,11			−8.21[n]	(6)s	

[a–f] As Table 6. [g] Note that $^{11}B(1)$ and $^{11}B(8)$ resonances (agglomerate peak 'A') are not resolved in the [^{11}B–^{11}B]-COSY spectrum. [h] Doublet, 24 Hz, ascribed to $^3J(^{31}P$–B–B–$^1H)$. [i] C_5Me_5 resonance position. [j] Cl-substituted site. [k] Doublet, 120 Hz, ascribed to $^1J(^{31}P$–$^{11}B)$. [l] PMe_2Ph-substituted site; P-methyl resonances at $\delta(^1H)$ *ca.* 1.96 and 1.91 p.p.m. [m] $^1J(^{11}B$–$^1H)$ coupling to H(7,11). [n] Doublet of doublets, 31.2 and 7.0 Hz, ascribed to $^1J(^{103}Rh$–$^1H)$ and $^2J(^{31}P$–B–$^1H)$ respectively.

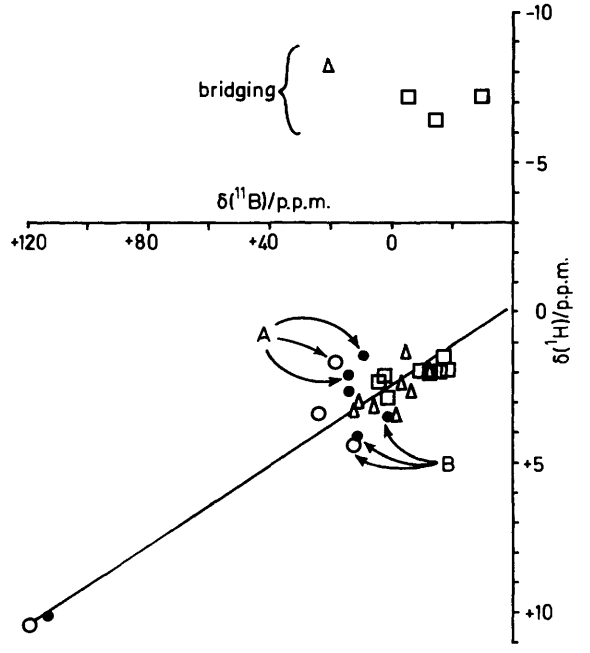

Figure 6. Plot of $\delta(^{11}B)$ against $\delta(^1H)$ for directly bound hydrogen atoms for compounds [(η^5-C_5Me_5)$RhB_{10}H_{10}$] (**1**) (○), [(η^5-C_5Me_5)-$RhB_{10}H_9(OMe)$] (**2**), (●), [(η^5-C_5Me_5)$RhB_{10}H_{11}Cl(PMe_2Ph)$] (**3**), (□), and [($\eta^5$-$C_5Me_5$)$RhOB_{10}H_9Cl(PMe_2Ph)$] (**4**) (△). The line drawn has slope $\delta(^1H)$:$\delta(^{11}B)$ 1:15, and points A and B are data for $^{11}B^1H(3,4,6,7)$ and $^{11}B^1H(8,10)$ respectively in compounds (**1**) and (**2**) (see text)

the large coupling $^1J(^{11}B$–$^1H)$ of 87 Hz from this boron atom to the Rh(7)–H–B(11) bridging hydrogen atom, this value being very large for a bridging configuration {*cf.*, for example, [6,6,6-$(PPh_3)_2$H-*nido*-6-RuB_9H_{12}-5-(PPh_3)] in ref. 37}. It was not possible to examine the non-oxygenated compound (**3**) for a comparable effect, however, because this species exhibited residual bridging-hydrogen atom fluxionality at the lowest temperatures at which its solutions remained in the liquid state, thus preventing the resolution of any coupling. Very recent results, however, indicate that triply bridged 7-molybda- and -tungsta-undecaboranes of *nido* configuration (**IX**) similarly exhibit large couplings $^1J(^{11}B$–$^1H)$ from B(8,11) to the M(7)–H–B(8,11) bridging hydrogen atoms (M = Mo or W).[26]

A plot of the boron-11 chemical shifts $\delta(^{11}B)$ *versus* the proton chemical shifts $\delta(^1H)$ for directly bound atoms in the new compounds (**1**)—(**4**) reported in this work is given in Figure 6. It is apparent for the compounds examined [apart from the diagnostic very low shielding associated with $^{11}B(2)$ and $^{11}B(5)$ for the *closo*-type species (**1**) and (**2**)] that there is a bunching of the boron chemical shifts in the central $\delta(^{11}B) = 0 \pm 20$ p.p.m. region. As observed for most larger contiguous polyhedral boron–hydride containing species,[34] there is a general parallel between the nuclear shielding of the boron atoms and their directly-bound *exo*-hydrogen atoms, the slope of the line drawn on the plot being $\delta(^1H)$:$\delta(^{11}B)$ 1:15 in this instance. Most of the (^{11}B,^1H)(*exo*) data are within 1 p.p.m. [in $\delta(^1H)$] from this line, although it is of interest to note that the data for the (3,4,6,7) (data A in Figure 6) and (8,10) positions (data B) in the *closo*-type compounds (**1**) and (**2**) are bunched respectively above and below this general correlation line. This is also apparent for other *closo*-type 1-metallaundecaboranes reported,[6–8,38] and is of use in assigning spectra. An important general consideration here is that linked (^{11}B,^1H) shielding behavioural patterns of this type have increasing use in spectroscopic assignments and thence structural characterization in polyhedral boron hydride chemistry without recourse to diffraction methods (for recent examples see refs. 18, 39, and 40).

Experimental

General.—Reactions were generally carried out under an atmosphere of dry nitrogen, subsequent manipulations and separations being carried out in air. The compounds [{Rh-(η^5-C_5Me_5)Cl_2}$_2$],[41] $B_{10}H_{12}(PMe_2Ph)_2$,[18] and salts of the $[B_{10}H_{10}]^{2-}$ anion[42] were prepared according to published methods. Preparative thin layer chromatography (t.l.c.) was carried out using 1-mm layers of silica (Kieselgel GF54; Fluka) on glass plates of dimensions 200 × 200 mm; these were prepared as required from an acetone slurry, followed by drying in air at *ca.* 80 °C.

Preparation of [(η^5-C_5Me_5)$RhB_{10}H_{10}$] (**1**).—A solution of [{Rh(η^5-C_5Me_5)Cl_2}$_2$] (0.1 g, 0.16 mmol) and [$NHEt_3$]$_2$-[$B_{10}H_{10}$] (0.1 g, 0.31 mmol) in CH_2Cl_2 (20 cm^3) was stirred for 30 min at room temperature. The resulting orange solution was

reduced to a smaller volume (*ca.* 5 cm^3) under reduced pressure (water pump) and chromatographed using CH_2Cl_2 as eluant. One coloured metallaborane component was present at R_f 0.8. This was recrystallized by addition of light petroleum (b.p. 60—80 °C) to a solution in CH_2Cl_2 to give bright orange crystals of compound (**1**) (51 mg, 0.14 mmol, 45%).

Preparation of $[(\eta^5\text{-}C_5Me_5)RhB_{10}H_9(OMe)]$ (**2**).—A solution of $[\{Rh(\eta^5\text{-}C_5Me_5)Cl_2\}_2]$ (0.15 g, 0.24 mmol) and $[NHEt_3]_2[B_{10}H_{10}]$ (0.155 g, (0.48 mmol) in MeOH (30 cm^3) was stirred for 15 min at room temperature, during which time the colour changed from red to bright orange. The volatile components were removed under reduced pressure (water pump) at *ca.* 50 °C the solid residue dissolved in CH_2Cl_2 (5 cm^3) and applied to preparative t.l.c. plates. Elution using CH_2Cl_2–hexane (50:50) gave two components, one orange with R_f 0.7, and one yellow with R_f 0.6. The orange component was crystallized from CH_2Cl_2 solution by the diffusion of hexane to give orange crystals of compound (**2**) (71 mg, 0.18 mmol, 37.5%). The yellow component is at present tentatively identified[9] as [5-(η^5-C_5Me_5)-*nido*-5-RhB_9H_{12}-6-X], where X = either Cl or OMe (15 mg, 0.04 mmol, 8%).

Preparation of $[(\eta^5\text{-}C_5Me_5)RhB_{10}H_{11}Cl(PMe_2Ph)]$ (**3**).—A suspension of $B_{10}H_{12}(PMe_2Ph)_2$ (0.253 g, 0.64 mmol) in a solution of $[\{Rh(\eta^5\text{-}C_5Me_5)Cl_2\}_2]$ (0.2 g, 0.32 mmol) in C_6H_6 (20 cm^3) was heated to reflux temperature and maintained there for 1 h. The resulting mixture was evaporated to dryness (water pump pressure) at *ca.* 30 °C, and dissolved in CH_2Cl_2 (*ca.* 10 cm^3). Preparative t.l.c. using 100% CH_2Cl_2 as eluting fluid gave colourless $B_{10}H_{12}(PMe_2Ph)_2$ (R_f 0.66; 117 mg, 0.30 mmol, 46% recovery) and a bright yellow component with R_f 0.44 that was recrystallized by diffusion of hexane into a solution of CH_2Cl_2 to give yellow crystals of compound (**3**) {45 mg, 0.07 mmol, 21% based on $[B_{10}H_{12}(PMe_2Ph)_2]$ consumed} as its 1:1 CH_2Cl_2 solvate. Other products of low chromatographic mobility under these conditions did not contain boron (as judged by n.m.r. spectroscopy).

Preparation of $[(\eta^5\text{-}C_5Me_5)RhOB_{10}H_9Cl(PMe_2Ph)]$ (**4**).—A suspension of $[(\eta^5\text{-}C_5Me_5)RhB_{10}H_{11}Cl(PMe_2Ph)]\cdot CH_2Cl_2$ (**3**) (0.1 g, 162 μmol) in CH_2Cl_2 (30 cm^3) that was saturated with H_2O, was stirred for 2 d at room temperature, during which time it formed a dark red solution. The volatile components were then removed under reduced pressure (water pump) at *ca.* 50 °C, the solid residue dissolved in CH_2Cl_2 (5 cm^3) and applied to preparative t.l.c. plates. Elution with 100% CH_2Cl_2 gave yellow (**3**) (R_f 0.44; 59 mg, 96 μmol, 59% recovery) and a red component with R_f 0.58. The latter was recrystallized from CH_2Cl_2 solution by the diffusion of hexane to yield red crystals of compound (**4**) [23 mg, 42 μmol, 63% based on (**3**) consumed]. Reaction under the same conditions, but with an excess of PMe_2Ph present, gave a similar yield of compound (**4**).

Crystallographic Studies.—All measurements were made using a Syntex $P2_1$ diffractometer operating in the ω—2θ scan mode using graphite monochromated Mo-K_α radiation (λ = 71.069 pm) following a procedure described elsewhere in detail.[43] The structures were solved *via* standard heavy-atom procedures and were refined by full-matrix least squares using

Table 10. Crystal data and details of refinement

Compound	(**2**)	(**3**)	(**4**)
(*a*) Crystal data			
Formula	$C_{11}H_{27}B_{10}ORh$	$C_{18}H_{37}B_{10}ClPRh\cdot CH_2Cl_2$	$C_{18}H_{35}B_{10}ClOPRh$
M	386.351	615.866	544.917
Crystal system	Triclinic	Monoclinic	Monoclinic
a/pm	1 407.7(2)	1 520.4(2)	867.7(2)
b/pm	878.9(1)	1 228.3(3)	1 984.4(4)
c/pm	835.9(2)	1 622.3(2)	1 551.8(3)
α/°	111.19(1)		
β/°	103.44(1)	102.24(1)	102.08(2)
γ/°	92.24(1)		
U/nm^3	0.929	2.937	2.613
Space group	$P\bar{1}$	$P2_1/n$	$P2_1/n$
Z	2	4	4
D_c/g cm^{-3}	1.38	1.39	1.38
μ(Mo-K_α)/cm^{-1}	8.18	8.25	7.43
F(000)	392	1 266	1 112
(*b*) Data collection			
Scan width/° below K_{α_1} to ° above K_{α_2}	1.0,1.0	1.0,1.0	1.0,1.0
Scan speed (min.,max.)/° min^{-1}	2.0,29.3	2.0,29.3	2.0,29.3
$2\theta_{min.,max.}$/°	4.0,45.0	4.0,45.0	4.0,50.0
Total data	3 367	4 334	5 212
Unique data	3 267	3 727	4 490
Observed data [$I > 2.0\sigma(I)$]	3 231	3 510	4 258
Temp./K	290	290	290
(*c*) Refinement			
Number of parameters	265	357	336
Weighting coefficient, *g*	0.0007	0.0001	0.0001
Final $R(= \Sigma\|\Delta F\|/\Sigma\|F_o\|)$	0.0270	0.0388	0.0407
Final $R'(= \Sigma w\|\Delta F\|^2/\Sigma\|F_o\|^2)$	0.0313	0.0432	0.0441

Table 11. Atom co-ordinates (× 10^4) for compound (**2**)

Atom	*x*	*y*	*z*
Rh(1)	7 644.2(1)	−330.9(2)	6 346.1(1)
C(1)	6 825(2)	−2 499(3)	6 508(3)
C(2)	6 948(2)	−2 940(3)	4 763(4)
C(3)	7 983(2)	−2 895(3)	4 911(3)
C(4)	8 482(2)	−2 338(3)	6 735(3)
C(5)	7 772(2)	−2 094(3)	7 731(3)
C(6)	5 859(2)	−2 695(4)	6 929(5)
C(7)	6 121(3)	−3 469(4)	3 098(4)
C(8)	8 445(3)	−3 574(4)	3 384(4)
C(9)	9 579(2)	−2 194(4)	7 478(5)
C(10)	7 987(3)	−1 666(4)	9 708(4)
B(2)	6 897(2)	1 282(3)	8 055(4)
B(3)	8 157(2)	2 212(4)	8 622(4)
B(4)	8 873(2)	1 804(4)	7 148(5)
B(5)	8 451(3)	453(4)	4 896(5)
B(6)	7 234(3)	940(4)	4 394(5)
B(7)	6 512(2)	1 346(4)	5 858(5)
B(8)	7 100(2)	3 172(4)	7 885(5)
B(9)	8 251(3)	3 596(4)	7 555(5)
B(10)	8 321(3)	2 474(4)	5 335(6)
B(11)	7 185(2)	3 024(4)	5 754(5)
O(21)	6 391(2)	862(2)	9 028(3)
C(21)	5 969(4)	2 032(5)	10 238(6)
H(3)	8 398(26)	2 383(41)	9 835(52)
H(4)	9 578(21)	1 571(33)	7 346(36)
H(5)	8 804(27)	−311(43)	3 882(47)
H(6)	6 984(30)	257(39)	3 431(46)
H(7)	5 824(27)	927(40)	5 366(46)
H(8)	6 764(18)	4 159(33)	8 610(35)
H(9)	8 757(23)	4 800(38)	8 377(43)
H(10)	8 533(49)	3 195(70)	4 834(36)
H(11)	6 981(28)	3 804(47)	5 492(51)

Table 12. Atom co-ordinates (× 10^4) for compound (**3**)

Atom	*x*	*y*	*z*
Rh(7)	9 803.6(2)	704.1(3)	2 071.2(2)
Cl(1)	11 308(1)	−1 496(1)	1 849(1)
P(1)	7 572(1)	1 896(5)	652(1)
C(11)	6 829(4)	2 013(5)	1 357(4)
C(12)	6 828(3)	1 652(4)	−389(3)
C(131)	8 037(2)	3 225(2)	541(2)
C(132)	8 570(2)	3 326(2)	−57(2)
C(133)	8 908(2)	4 342(2)	−217(2)
C(134)	8 713(2)	5 258(2)	221(2)
C(135)	8 180(2)	5 157(2)	819(2)
C(136)	7 842(2)	4 141(2)	979(2)
C(1)	10 516(3)	2 295(4)	2 393(3)
C(2)	11 138(3)	1 428(4)	2 653(3)
C(3)	10 838(4)	771(4)	3 262(3)
C(4)	10 019(3)	1 254(4)	3 383(3)
C(5)	9 820(3)	2 194(4)	2 849(3)
C(6)	10 614(4)	3 204(4)	1 801(4)
C(7)	12 013(3)	1 273(6)	2 396(4)
C(8)	11 362(5)	−134(5)	3 788(4)
C(9)	9 504(5)	882(6)	4 014(4)
C(10)	9 103(4)	3 003(5)	2 878(4)
B(1)	8 320(4)	−1 468(5)	1 625(4)
B(2)	8 436(4)	−70(5)	1 927(3)
B(3)	9 393(4)	−1 008(5)	2 220(3)
B(4)	9 301(4)	−1 918(4)	1 345(3)
B(5)	8 331(4)	−1 623(4)	524(3)
B(6)	7 813(4)	−481(5)	886(3)
B(8)	10 152(3)	−930(4)	1 512(3)
B(9)	9 420(4)	−1 251(4)	420(3)
B(10)	8 434(4)	−305(4)	113(3)
B(11)	8 440(3)	724(4)	974(3)
H(1)	7 924(30)	−1 986(37)	1 908(28)
H(2)	8 106(23)	264(29)	2 421(21)
H(3)	9 678(25)	−1 382(31)	2 896(24)
H(4)	9 518(30)	−2 798(38)	1 437(28)
H(5)	8 966(34)	−2 307(43)	153(32)
H(6)	7 171(38)	−368(40)	689(32)
H(9)	9 721(27)	−1 649(34)	−41(27)
H(10)	8 135(26)	−66(34)	−562(25)
H(7,8)	10 203(25)	12(33)	1 283(23)
H(7,11)	9 207(30)	1 017(36)	1 001(27)
H(9,10)	9 232(28)	−271(33)	215(24)

Table 13. Atom co-ordinates (× 10^4) for compound (**4**)

Atom	*x*	*y*	*z*
Rh(7)	1 218.0(3)	1 669.5(1)	3 878.6(2)
Cl(8)	−288(2)	3 236(1)	4 365(1)
P(1)	1 556(1)	1 045(1)	1 649(1)
O(12)	203(3)	2 890(1)	2 740(2)
C(11)	1 605(6)	1 380(3)	568(3)
C(12)	3 178(5)	468(3)	1 907(4)
C(131)	−252(2)	576(1)	1 477(1)
C(132)	−1 655(2)	929(1)	1 185(1)
C(133)	−3 092(2)	587(1)	1 029(1)
C(134)	−3 127(2)	−107(1)	1 165(1)
C(135)	−1 724(2)	−460(1)	1 458(1)
C(136)	−287(2)	−118(1)	1 613(1)
C(1)	1 130(4)	612(2)	4 332(2)
C(2)	−423(4)	873(2)	4 154(2)
C(3)	−486(4)	1 423(2)	4 746(2)
C(4)	1 055(4)	1 511(2)	5 266(2)
C(5)	2 071(4)	1 014(2)	5 010(2)
C(6)	1 686(6)	−25(2)	3 960(3)
C(7)	−1 828(5)	585(2)	3 533(3)
C(8)	−1 959(5)	1 792(2)	4 846(3)
C(9)	1 498(5)	1 984(2)	6 039(3)
C(10)	3 775(5)	909(2)	5 425(3)
B(1)	4 108(5)	2 715(3)	3 393(3)
B(2)	3 391(5)	1 858(2)	3 412(3)
B(3)	2 904(5)	2 502(2)	4 147(3)
B(4)	2 814(6)	3 320(2)	3 646(3)
B(5)	2 980(6)	3 198(2)	2 550(3)
B(6)	3 135(5)	2 317(2)	2 393(3)
B(8)	972(5)	2 833(2)	3 712(3)
B(9)	1 235(6)	3 484(3)	2 771(3)
B(10)	1 213(5)	2 681(2)	2 082(3)
B(11)	1 726(5)	1 743(2)	2 545(3)
H(1)	5 345(13)	2 859(11)	3 624(12)
H(2)	4 284(13)	1 463(12)	3 561(12)
H(3)	3 647(13)	2 541(11)	4 900(12)
H(4)	3 247(13)	3 762(12)	4 085(12)
H(5)	3 570(13)	3 537(12)	2 124(12)
H(6)	3 687(13)	2 197(11)	1 826(12)
H(9)	620(13)	4 021(11)	2 556(12)
H(10)	538(13)	2 693(11)	1 394(12)
H(7,11)	409(13)	1 791(11)	2 740(12)

the SHELX program system.[44] All three data sets were corrected for absorption empirically once their structures had been determined.[45]

Refinement of all three structures was basically the same with all non-hydrogen atoms assigned anisotropic thermal parameters, except for those in the CH_2Cl_2 solvent of compound (**3**) which were assigned an overall isotropic thermal parameter. All methyl and phenyl hydrogen atoms were included in calculated positions (C–H = 108 pm) and assigned to an overall isotropic thermal parameter for each group. All borane cluster hydrogen atoms were located experimentally and were freely refined with individual isotropic thermal parameters. The weighting scheme

Table 14. Experimental details for the two-dimensional [^{11}B–^{11}B]- and [^{1}H–^{1}H]-COSY experiments

Compound	(1)	(2)	(3)	(4)	(3)	(4)
COSY experiment	[^{11}B–^{11}B]	[^{11}B–^{11}B]	[^{11}B–^{11}B]	[^{11}B–^{11}B]	[^{1}H–^{1}H]	[^{1}H–^{1}H]
Data size (t_2,t_1/words)	256,128	256,128	512,128	512,128	1 024,256	1 024,256
Transform size (F_2,F_1/words)	512,256	512,256	512,256	512,256	1 024,512	1 024,512
t_2 sweep width (= 2 × t_1 sweepwidth/Hz)	17 214	18 518	7 246	7 143	4 950	7 042
Digital resolution (Hz/pt)	148/2	152/2	28	28	10	14
No. of transients per t_1 increment	256	128	4 000	2 600	80	96
Recycling time (s)	0.02	0.02	0.05	0.08	2.1	2.1
Mixing pulse (°)	90	45	45	90	90	90

$w = [\sigma^2(F_o) + g(F_o)^2]^{-1}$ was used at the end of refinement for all three structures, in which the variable g was included in the refinement in order to obtain acceptable agreement analyses.

Details of the crystal data, intensity measurements, and refinements are given in Table 10. Atomic co-ordinates for compounds (**2**), (**3**), and (**4**) are given in Tables 11, 12, and 13 respectively.

Nuclear Magnetic Resonance Spectroscopy.—Experiments were performed at 2.35 or 9.40 T on commercially available instrumentation. Chemical shifts $\delta(^1H)$, $\delta(^{31}P)$, and $\delta(^{11}B)$ are given to high frequency (low field) of Ξ100 MHz (internal $SiMe_4$), Ξ40.480 730 MHz (nominally 85% H_3PO_4), and Ξ32.083 971 MHz [nominally $BF_3(OEt_2)$ in $CDCl_3$],[34] respectively, measured in each case using residual deuteriated solvent proton resonances as internal secondary standards. The selective ^1H-{^{11}B} technique has been adequately described elsewhere,[18,32,33,46] use being made of the procedure in which the ^1H-{^{11}B(off-resonance)} spectrum is subtracted from the ^1H-{^{11}B(on-resonance)} spectrum in order to remove lines arising from protons which are not coupled to the ^{11}B nucleus of interest.[33,47] Other 'one-dimensional' spectroscopy was otherwise straightforward. 'Two-dimensional' spectroscopy was performed at 9.40 T. The two-dimensional [^{11}B–^{11}B]-COSY[28–30] experiments were acquired with a 90° [(**1**) and (**4**)] or a 45° [(**2**) and (**3**)] mixing pulse using, typically, 512 and 128 words of data in the t_2 and t_1 dimensions respectively. The total experimental times varied from *ca.* 15 min [(**1**) and (**2**)] to *ca.* 8 h [(**3**) and (**4**)], uninterrupted {^{1}H(broad-band noise)} decoupling being applied throughout. The two-dimensional [^{1}H–^{1}H]-COSY[31] experiments were acquired with a 90° mixing pulse, using 1 024 and 256 words of data in the t_2 and t_1 dimensions respectively. With a relaxation delay of 2 s the total experimental times were *ca.* 12 h; uninterrupted {^{11}B(broad-band noise)} decoupling was applied throughout. The two-dimensional time domain matrices were weighted with an unshifted sine bell apodization function prior to Fourier transformation. The frequency domain matrices were symmetrized along their ($F_1 = F_2$) diagonals. Precise experimental details for the two-dimensional COSY results in Tables 1, 6, and 9 are given in Table 14.

Acknowledgements

We thank the S.E.R.C. for support.

References

1 Part 1, X. L. R. Fontaine, H. Fowkes, N. N. Greenwood, J. D. Kennedy, and M. Thornton-Pett, *J. Chem. Soc., Dalton Trans.*, 1986, 547.
2 Part 2, X. L. R. Fontaine, H. Fowkes, N. N. Greenwood, J. D. Kennedy, and M. Thornton-Pett, *J. Chem. Soc., Dalton Trans.*, 1987, 1431.
3 X. L. R. Fontaine, H. Fowkes, N. N. Greenwood, J. D. Kennedy, and M. Thornton-Pett, *J. Chem. Soc., Chem. Commun.*, 1985, 1165.
4 X. L. R. Fontaine, H. Fowkes, N. N. Greenwood, J. D. Kennedy, and M. Thornton-Pett, *J. Chem. Soc., Chem. Commun.*, 1985, 1722.
5 R. N. Grimes, in 'Comprehensive Organometallic Chemistry,' eds. G. Wilkinson, F. G. A. Stone, and E. Abel, Pergamon, Oxford, 1982, Part I, ch. 5.5, p. 471, Figure 14.
6 H. Fowkes, N. N. Greenwood, J. D. Kennedy, and M. Thornton-Pett, *J. Chem. Soc., Dalton Trans.*, 1986, 517.
7 J. E. Crook, M. Elrington, N. N. Greenwood, J. D. Kennedy, M. Thornton-Pett, and J. D. Woollins, *J. Chem. Soc., Dalton Trans.*, 1985, 2407.
8 M. Elrington, Ph.D. Thesis, University of Leeds, 1985.
9 M. Bown, X. L. R. Fontaine, H. Fowkes, N. N. Greenwood, J. D. Kennedy, P. MacKinnon, K. Nestor, and M. Thornton-Pett, unpublished work, University of Leeds, 1984—1986.
10 R. P. Micciche, J. J. Briguglio, and L. G. Sneddon, *Inorg. Chem.*, 1984, **23**, 3992.
11 See, for example, J. J. Briguglio and L. G. Sneddon, *Organometallics*, 1986, **5**, 327 and refs. therein.
12 K. Wade, *Chem. Commun.*, 1971, 792; *Adv. Inorg. Chem. Radiochem.*, 1976, **18**, 1.
13 R. E. Williams, *Inorg. Chem.*, 1971, **10**, 210; *Adv. Inorg. Chem. Radiochem.*, 1976, **18**, 67.
14 J. E. Crook, M. Elrington, N. N. Greenwood, J. D. Kennedy, and J. D. Woollins, *Polyhedron*, 1984, **3**, 901.
15 R. T. Baker, *Inorg. Chem.*, 1986, **25**, 109.
16 J. D. Kennedy, *Inorg. Chem.*, 1986, **25**, 111.
17 C. W. Jung and M. F. Hawthorne, *J. Am. Chem. Soc.*, 1980, **102**, 3024.
18 X. L. R. Fontaine and J. D. Kennedy, *J. Chem. Soc., Dalton Trans.*, 1987, 1573 and refs. therein.
19 G. Fergusson, M. F. Hawthorne, B. Kaitner, and F. J. Lalor, *Acta Crystallogr., Sect. C*, 1984, **40**, 1707.
20 J. D. Kennedy, *Prog. Inorg. Chem.*, 1984, **32**, 519; 1986, **34**, 211 and refs. therein.
21 X. L. R. Fontaine, N. N. Greenwood, J. D. Kennedy, P. MacKinnon, and M. Thornton-Pett, *J. Chem. Soc., Chem. Commun.*, 1986, 1111.
22 T. L. Venable and R. N. Grimes, *Inorg. Chem.*, 1982, **21**, 887.
23 T. L. Venable, E. Sinn, and R. N. Grimes, *Inorg. Chem.*, 1982, **21**, 895.
24 T. L. Venable, E. Sinn, and R. N. Grimes, *J. Chem. Soc., Dalton Trans.*, 1984, 2275.
25 M. Bown, X. L. R. Fontaine, N. N. Greenwood, J. D. Kennedy, and M. Thornton-Pett, *J. Chem. Soc., Dalton Trans.*, 1987, 1169.
26 X. L. R. Fontaine, N. N. Greenwood, J. D. Kennedy, I. Macpherson, and M. Thornton-Pett, unpublished work; I. Macpherson, Ph.D. Thesis, University of Leeds, 1987.
27 R. N. Leyden, B. P. Sullivan, R. T. Baker, and M. F. Hawthorne, *J. Am. Chem. Soc.*, 1978, **100**, 3758.
28 T. L. Venable, W. C. Hutton, and R. N. Grimes, *J. Am. Chem. Soc.*, 1982, **104**, 4716; 1984, **106**, 209.
29 I. J. Colquhoun and W. McFarlane, results presented to 'The First and Third National Meetings of British Inorganic Boron Chemists,' INTRABORON I, Strathclyde, May 1980, and INTRABORON III, Leeds, September 1982.
30 D. Reed, *J. Chem. Res. (S)*, 1984, 198.
31 X. L. R. Fontaine and J. D. Kennedy, *J. Chem. Soc., Chem. Commun.*, 1986, 779.
32 J. D. Kennedy and B. Wrackmeyer, *J. Magn. Reson.*, 1980, **38**, 529.
33 S. K. Boocock, N. N. Greenwood, M. J. Hails, J. D. Kennedy, and W. S. McDonald, *J. Chem. Soc., Dalton Trans.*, 1981, 1415.
34 J. D. Kennedy, in 'Multinuclear N.M.R.,' ed. J. Mason, Plenum, London and New York, 1987, ch. 8, pp. 221—258 and refs. therein.

35 See, for example, M. A. Beckett and J. D. Kennedy, *J. Chem. Soc., Chem. Commun.*, 1983, 575.
36 See, for example, R. R. Rietz, A. R. Siedle, R. O. Schaeffer, and L. J. Todd, *Inorg. Chem.*, 1973, **12**, 2100.
37 N. N. Greenwood, J. D. Kennedy, M. Thornton-Pett, and J. D. Woollins, *J. Chem. Soc., Dalton Trans.*, 1985, 2397.
38 M. Elrington, N. N. Greenwood, J. D. Kennedy, and M. Thornton-Pett, *J. Chem. Soc., Dalton Trans.*, 1986, 2277.
39 M. A. Beckett, M. Bown, X. L. R. Fontaine, N. N. Greenwood, J. D. Kennedy, and M. Thornton-Pett, unpublished work.
40 N. N. Greenwood, J. D. Kennedy, I. Macpherson, and M. Thornton-Pett, *Z. Anorg. Allg. Chem.*, 1986, **540/541**, 45.
41 J. W. Kang, K. Mosely, and P. M. Maitlis, *J. Am. Chem. Soc.*, 1969, **91**, 5970.
42 M. F. Hawthorne and A. R. Pittochelli, *J. Am. Chem. Soc.*, 1969, **91**, 5519; M. F. Hawthorne, R. L. Pilling, and R. N. Grimes, *ibid.*, 1964, **86**, 5338; M. F. Hawthorne and R. L. Pilling, *Inorg. Synth.*, 1967, **9**, 16.
43 A. Modinos and P. Woodward, *J. Chem. Soc., Dalton Trans.*, 1974, 2065.
44 G. M. Sheldrick, SHELX 76, Program System for *X*-Ray Structure Determination, University of Cambridge, 1976.
45 N. Walker and D. Stuart, *Acta Crystallogr., Sect. A*, 1983, **39**, 158.
46 J. D. Kennedy and N. N. Greenwood, *Inorg. Chim. Acta*, 1980, **38**, 93.
47 J. D. Kennedy and J. Staves, *Z. Naturforsch., Teil B*, 1979, **34**, 808.

Received 17*th September* 1986; *Paper* 6/1840